Defect Detection in Textile Fabric Images Using Subband Domain Subspace Analysis

A. Serdaroglu[a], A. Ertuzun[a], and A. Ercil[b]

[a] *Boğaziçi University, Electrical and Electronics Engineering Department, Istanbul, Turkey*
[b] *Sabanc@ University, Faculty of Engineering and Natural Sciences, Istanbul, Turkey*
e-mail: serdaroa@boun.edu.tr, ertuz@boun.edu.tr, aytulercil@sabanciuniv.edu

Abstract—In this work, a new model that combines the concepts of wavelet transformation and subspace analysis tools, like independent component analysis (ICA), topographic independent component analysis (TICA), and Independent Subspace Analysis (ISA), is developed for the purpose of defect detection in textile images. In previous works, it has been shown that reduction of the textural components of the textile image by preprocessing has increased the performance of the system. Based on this observation, in the present work, the aforementioned subspace analysis tools are applied to subband images. The feature vector of a subwindow of a test image is compared with that of a defect-free image in order to make a decision. This decision is based on a Euclidean distance classifier. The increase performance that results from using wavelet transformation prior to subspace analysis has been discussed in detail. While it has been found that all subspace analysis methods lead to the same detection performances, as a further step, independent subspace analysis is used to classify the detected defects according to their directionalities.

DOI: 10.1134/S105466180704027X

1. INTRODUCTION

Automated industrial inspection systems based on hardware and/or software tools have been very successful in application to on-line quality control applications by virtue of their ability to make repetitive measurements accurately, fast, and objectively. One of the industry fields where automated visual inspection systems are mostly needed is the textile industry. Especially, the quality control of products in the textile industry is a significant problem, while the detection of defects in a fabric quality control system with a width of 1.60–2.0 m and which moves with an average speed of 10 m per minute is difficult for human observers. Thus, automated visual inspection systems play a great role in assessing the quality of fabrics. Other than classifying a certain appearance of the fabric, detection of the exact location of the defects and determination of their type are also important in some applications. An important point for the manufacturer is to get a warning when a certain amount of anomalies or imperfections occur during the production of fabric so that necessary precautions can be taken before the product reaches the market.

Texture analysis plays an important role in the automated visual inspection of surfaces. There have been number of works on the use of texture analysis for inspection purposes by artificial visual methods. Amet et al. [1] have used subband domain cooccurrence matrices for texture defect detection; Karras et al. [18] have suggested focusing on detecting defects from the wavelet transformation of images and to vector-quantizing related properties of the associated wavelet coefficients. Chen and Jain [6] used a structural approach to detecting defects in textured images. Dewaele et al. [9] used signal processing methods to detect point defects and line defects in texture images. Cohen et al. [7] used MRF models for inspecting defects of textile surfaces, while Ercil et al. [10] used similar techniques for inspection of painted metallic surfaces. Atalay [2] has implemented an MRF model-based method on a TMS320C40 parallel processing system for real-time defect inspection of textile fabrics. Lambert et al. [20] introduced an approach to exploit multiscale wavelet methods for texture defect detection, whereas Meylani et al. [23, 24] used lattice filters for the same purpose. Iivarinen [17] compared the performances of histogram-based texture analysis techniques, namely, the cooccurence matrix method and the local binary pattern method for surface defect detection. Bodnarova et al. [3] computed the parameters of a Gabor filter through optimization of the Fisher cost function and constrained these parameters to specific values to detect specific defects. Chan and Pang [5] used a three-dimensional frequency spectrum for the analysis of defects. For surveys of texture analysis, see Van Gool et al. [31], Reed et al. [26], Rao [25], and Tuceryan and Jain [30]. The first application of independent component analysis (ICA) on image data was the pioneering work of Hurri [11], in which he examined the general characteristics of independent components of texture images. Some preliminary results on the use of ICA for defect detection are presented in [27–29].

Received March 23, 2005

In this work, we propose a new defect detection algorithm based on ICA of subband images obtained by decomposing the original texture images. Wavelets are shown [22] to form a complete basis for multiresolution representation of images. Wavelet transform analysis facilitates inspection of the spatial–spatial-frequency contents of a signal in a unified framework. This constitutes the background for their use in texture analysis.

Our work is intended to be a continuation of the studies conducted by Amet et al. [1], and Sezer et al. [28]. In [1], a method that depends on the principle of decomposing grayscale images into their subbands using the pyramid structured wavelet transform (PSWT) and wavelet packet signatures (WPSs), and then extracting the cooccurrence properties using these subband images, was built. In [28], Sezer et al. increased defect detection performance by applying certain preprocessing methods like median filtering and histogram modification on the textile fabric images before applying ICA. These two works announced the idea that decomposing a textile fabric image into its subbands by wavelet transforms as a preprocessing step and applying ICA on these subbands will increase performance. A previous work by Serdaroglu et al. showed that defect detection performance in textile fabric images improved when the concepts of wavelet transformation were combined with ICA [27].

In this paper, we have conducted several experiments with combining wavelet transformation and ICA. We also investigated topographic independent component analysis (TICA) and independent subspace analysis (ISA) as a feature extraction step on these subbands. General concepts about ICA, TICA, and ISA are provided in Section 2. Section 3 gives a short explanation about the theory of wavelet transforms and wavelet packets. The methodologies used to conduct the experiments are explained in Section 4. Section 5 describes the performed experiments, and Section 6 concludes the paper.

2. SUBSPACE ANALYSIS METHODS

2.1. Independent Component Analysis

ICA has the goal of finding a linear transformation of original data such that the new representation minimizes the statistical dependence of the components of the representation. In other words, ICA tries to find the hidden components inside the original data, and these components capture the essential structure of the data. The representation achieved by ICA facilitates the analysis of the data encountered in such fields like data compression, pattern recognition, denoising, etc. [12, 13].

Transformation methods like principal component analysis (PCA), factor analysis, and projection pursuit are closely related to ICA. As in projection pursuit, ICA tries to find the *interesting directions* that give the independent components. ICA can also be considered as a *nongaussian factor analysis*. Both PCA and ICA formulate an objective function in order to define a linear representation and then maximize that function. From this perspective, PCA and ICA appear similar; however, they define their objective functions in very different ways. While PCA uses second-order statistics in order to find the principal components, ICA needs higher order statistics in order to find the independent components. A much stronger relation can be seen between ICA and nonlinear principal component analysis (NLPCA) [32]. In [32], Xu uses the concept of least mean square error reconstruction (LMSER) in order to estimate the nonlinear principal components. It turns out that the nonlinear principal components are, in some cases, aligned with the independent components of the input data.

The basic ICA model is given as [12, 13]

$$\mathbf{x} = \mathbf{A}\mathbf{s}, \tag{2.1}$$

where x is a random vector containing the mixtures, $\mathbf{s}$ is a random vector containing the independent sources, and $\mathbf{A}$ is the mixing matrix. No a priori information about the mixing matrix or the sources is known. These sources can be different parts of the brain emitting different signals, people speaking at a cocktail party so that many speech signals are emitted, different mobile phones radiating different electromagnetic signals from their antennas, or some other sources that are not known but are assumed to exist that are somehow producing the observed signals. In order to estimate the independent components by observing the mixtures $\mathbf{x}$, the sources $\mathbf{s}$ must be assumed to be independent from each other, with each having a nongaussian probability distribution. The sources $\mathbf{s}$ can be estimated after finding the demixing matrix $\mathbf{B}$, given in Eq. (2.2):

$$\mathbf{s} = \mathbf{B}\mathbf{x}, \tag{2.2}$$

where $\mathbf{B}$ is the (pseudo) inverse of $\mathbf{A}$.

These estimated sources are called *independent components*. The ICA model can estimate the independent components up to such ambiguities as scaling and ordering. The scaling problem can be solved by restricting the variances of the independent components to unity. However, there still remains a sign ambiguity, which is not a problem in many cases. In order to solve the ordering problem, certain ordering methods have been advised in [12, 13].

The demixing matrix can be estimated by maximization of the nongaussianity of the sources [12, 13]. Using the approximation of the negentropy or kurtosis in measuring the nongaussianity of data, a corresponding cost function can be built and maximized by either the gradient ascent method or by a fixed point algorithm.

There are two standard preprocessing steps, centering and whitening, that are used in ICA [12, 13]. These steps are applied in order to make ICA estimation better

conditioned and simpler; hence they do not change the ICA model given in Eq. (2.1). After whitening of the data, which can be achieved by PCA, the independent sources can be obtained as

$$\mathbf{s} = \mathbf{W}\mathbf{z}, \tag{2.3}$$

where $\mathbf{W}$ is the whitened demixing matrix that we are attempting to estimate and $\mathbf{z}$ is the whitened data. After finding $\mathbf{W}$, the estimation of the original mixing matrix $\mathbf{A}$ can be performed using Eq. (2.4):

$$\mathbf{A} = \mathbf{E}\mathbf{D}^{1/2}\mathbf{W}^{\mathrm{T}}, \tag{2.4}$$

where $\mathbf{D}$ is a diagonal matrix consisting of the eigenvalues of the correlation matrix of $\mathbf{x}$ and $\mathbf{E}$ is the matrix of corresponding eigenvectors. So, only the estimation of the rows of $\mathbf{W}$ is left to be done. As mentioned before, this is achieved by maximizing the nongaussianity of the data. In order to maximize nongaussianity, either the absolute value of the kurtosis or the negentropy can be maximized [12, 13]. Then the rows of the demixing matrix can be updated using a gradient-based algorithm or a fixed-point algorithm [14].

2.2. Topographic Independent Component Analysis

In ordinary ICA, the components are assumed to be independent. However, the estimated independent components are not often statistically independent. In fact, it is not possible, in general, to decompose a random vector x linearly into components that are perfectly independent. One of the possible solutions to this problem is to relax the independence assumption and to use the dependence of the neighboring independent components as a way to develop new tools for feature extraction. Multidimensional ICA [4], ISA [15], and TICA [16] are concepts that have been built using this independence relaxation idea.

In TICA, an independent component is made dependent with its neighboring independent components according to a predefined topographic neighborhood scheme. In this way, an ordering of the independent components in terms of dependences can be achieved. The dependency between nearby components is modeled by correlation of energies, which is a certain kind of high-order correlation. This means that

$$\mathrm{cov}(s_i^2, s_j^2) = E\{s_i^2 s_j^2\} - E\{s_i^2\}E\{s_j^2\} \neq 0 \tag{2.5}$$

if s_i and s_j are close in topography.

The topography scheme is defined according to a predefined 1D or 2D neighborhood function. A simple one-dimensional topography can be defined by the following neighborhood function [16]:

$$\mathrm{neigh}(i, j) = \begin{cases} 1, & \text{if } |i - j| \leq m \\ 0, & \text{otherwise.} \end{cases} \tag{2.6}$$

The learning rule can be defined as in Eqs. (2.7) and (2.8), where the ith row vector $\mathbf{w}_i$ of $\mathbf{W}$ is updated by a gradient algorithm:

$$\Delta\mathbf{w}_i \propto E\{\mathbf{z}(\mathbf{w}_i^T\mathbf{z})\mathbf{r}_i\}, \tag{2.7}$$

where

$$r_i = \sum_{k=1}^{n} \mathrm{neigh}(i, k)\, g\left(\sum_{j=1}^{n} \mathrm{neigh}(k, j)(w_j^T z)^2\right). \tag{2.8}$$

The vectors w_i must be normalized to unit variance and orthogonalized after every step.

2.3. Independent Subspace Analysis

In ISA [15], on the other hand, some dependences between the components are modeled. It combines the concepts of multidimensional ICA [4] with the principle of invariant-feature subspaces [19].

2.3.1 Invariant-feature subspaces. In the classical approaches of feature extraction, the presence of a given feature is detected taking the dot product of input data with a given feature vector. Linear features found in this way have the disadvantage of no invariance with respect to spatial shift or change in phase. Kohonen [19] developed the concept of invariant-feature subspaces in order to represent features with some invari- 5
ances.

2.3.2 Multidimensional ICA. In multidimensional independent component analysis, [4], it is assumed that the independent components, s_i, can be divided into couples, triplets, or in general, n-tuples, such that the s_i inside a given n-tuple may be dependent on each other, but dependences among different n-tuples are not allowed.

In order to combine the concepts of invariant-feature subspaces and multidimensional ICA, the probability distributions of the n-tuples of the independent components s_i that are taken to be spherically symmetric; i.e., they depend only on the norm. So, the logarithm of the likelihood L of the data, that is, the K observed image subwindows (or patches) $I_k(x, y)$, $k = 1, \ldots, K$, given the model, can be expressed as follows:

$$\log L(I_k(x, y), k = 1, \ldots, K; \mathbf{w}_i(x, y), i = 1, \ldots, m) = \sum_{k=1}^{k}\sum_{j=1}^{j} \log p\left(\sum_{i \in S_j} \langle \mathbf{w}_i, I_k\rangle^2\right) + K\log|\det\mathbf{W}|, \tag{2.9}$$

where $p(\sum_{i \in S_j} s_i^2) = p_j(s_i, i \in S_j)$ gives the probability density inside the jth n-tuple of s_i. J is the number of subspace groups. $\mathbf{w}_i$ are the rows of the demixing matrix $\mathbf{W}$. Since a prewhitening is done, $\mathbf{W}$ is an 6
orthogonal matrix; therefore, the second term in the above summation is zero.

By gradient ascent of the log likelihood given in Eq. (2.9), the learning algorithm for the extraction of independent subspaces can be obtained. The vectors $\mathbf{w}_i$ are constrained to be orthogonal and of unit norm, as in ordinary ICA. The learning rule for ISA can be stated as in Eq. (2.10):

$$Dw_i(x, y) \alpha I(x, y) \langle w_i, I \rangle g\left(\sum_{r \subset S_{j(i)}} \langle w_r, I \rangle^2 \right), \quad (2.10)$$

where $j(i)$ is the index of the subspace to which $\mathbf{w}_i$ belongs and $g = p'/p$ is a nonlinear function.

2.4. Independent Components of Images

In this project, our goal is to find the independent components of textile fabric images for the purpose of defect detection. In the work by Hurri et al. [11], subwindows from images are taken in order to form the samples of the data vector **x**. Each pixel of the image subwindow is a random variable, and as the number of image subwindows taken from images is increased, we can get a more thorough picture of the statistics of that random variable. The aim of ICA is to make these image pixels as mutually independent as possible.

An image subwindow $I(x, y)$ can be represented as a linear sum of its basis functions (i.e. independent components) which can be extracted by ICA (or TICA or ISA).

$$I(x, y) = \sum_{i=1}^{n} a_i(x, y) s_i. \quad (2.11)$$

Here, $a_i(x, y)$ are called *basis functions*, and the s_i constitute the feature vector used in the proposed defect detection system.

3. WAVELET TRANSFORMS

Wavelet transformation is a tool used to decompose a signal into its subbands. The advantages of multiresolution analysis have been widely investigated. Any signal can be decomposed into multiple frequency bands using a single set of filter coefficients. Furthermore, wavelet transforms have good spatial–spatial-frequency localization. Directional information is inherent in wavelet coefficients. Namely the LH, HL and HH bands contain details in the horizontal, vertical and diagonal directions respectively.

Wavelets, although known for many years, received the attention of the image processing society only after the papers by Daubechies [8], who provided the discretization of the wavelet transform, and Mallat [22], who established the connection between multiresolution theory and wavelet transforms.

In this section, the background theory about discrete wavelet transform and decomposition of a signal using wavelet filters are given. By virtue of the translations and dilation of a function represented as $\psi(t)$ and known as the *mother wavelet*, one can obtain a family of orthonormal basis functions. These bases are represented as $\psi_{m,n}(t)$, and the decomposition of a signal is performed with these bases. The construction of the basis function from the mother wavelet can be represented by the following formula:

$$\psi_{m,n}(t) = 2^{-m/2} \psi(2^{-m} t - n). \quad (3.1)$$

The analysis and synthesis formulas for a signal $x(t)$ are given as follows:

$$c_{m,n} = \int_{-\infty}^{+\infty} x(t) \psi_{m,n}(t) dt, \quad (3.2)$$

$$x(t) = \sum_{m,n} c_{m,n} \psi_{m,n}(t). \quad (3.3)$$

For the construction of the mother wavelet, a function known as *scaling function* $\phi_{m,n}(t)$, is used:

$$\phi_{m,n}(t) = \sqrt{2} \sum_{k} g_0(k) \phi_{m,n}(2t - k). \quad (3.4)$$

Then $\psi_{m,n}$ is found as follows

$$\psi_{m,n}(t) = \sqrt{2} \sum_{k} g_1(k) \phi_{m,n}(2t - k). \quad (3.5)$$

Here $g_0(n)$ and $g_1(n)$ are called the *reconstruction low-pass filter* and *reconstruction high-pass filter*, respectively. Their mutual relation can be given by

$$g_1(k) = (-1)^k g_0(1 - k). \quad (3.6)$$

The transformation coefficients can be obtained recursively; there is no need to explicitly calculate the scaling and mother wavelet functions. J-level decomposition can be written as in Eqs. (3.7) to (3.9):

$$x(t) = \sum_{k} \left(c_{J+1,k} \phi_{J+1,k}(k) + \sum_{j=0}^{J} d_{j+1,k} \Psi_{j+1,k}(t) \right), \quad (3.7)$$

where

$$c_{j+1,n} = \sum_{k} c_{j,k} g_0(k - 2n) \quad (3.8)$$

and

$$d_{j+1,n} = \sum_{k} d_{j,k} g_1(k - 2n) \quad (3.9)$$

for $0 \le j \le J$. Equations (3.8) and (3.9) are in fact the convolution of coefficients $c_{j,n}$ and $d_{j,n}$ at resolution j with filters h_0 and $h_1(n)$, then down-sampling by two to obtain $c_{j+1,n}$ and $d_{j+1,n}$. The coefficients $c_{j,n}$ are called

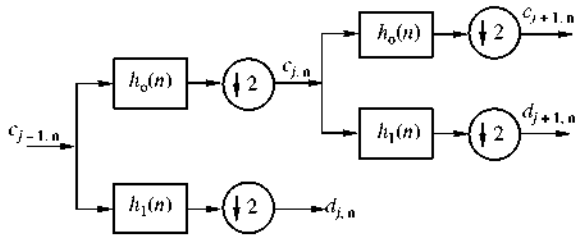

Fig. 1. Two-level wavelet decomposition diagram.

AA	*AH*	*HA*	*HH*
AV	*AD*	*HV*	*HD*
VA	*VH*	*DA*	*DH*
VV	*VD*	*DV*	*DD*

Fig. 2. Two-dimensional wavelet packet tree decomposition.

low-resolution coefficients, and the coefficients $d_{j,n}$ are called *detail coefficients*. $h_0(n)$ is the *decomposition low-pass filter*, and $h_1(n)$ is the *decomposition high-pass filter*. They have a mutual relationship given as

$$h_0(n) = g_0(-n), \quad h_1(n) = g_1(-n) \qquad (3.10)$$

Decomposition: The output of J-level decomposition will contain the low-resolution coefficient $c_{J,n}$ and detail coefficients $d_{j,n}$ for each level $(1 \le j \le J)$. The decomposition scheme is shown in the Fig. 1.

Synthesis: The procedure works opposite to this case. The low-resolution coefficient $c_{J,n}$ and detail coefficients $d_{j,n}$ are first upsampled and then filtered with the reconstruction low-pass and high-pass filters $g_0(n)$ and $g_1(n)$, respectively.

3.1. Wavelet Packets

The decomposition of a signal can be performed via the conventional method of wavelet transform and is called the *pyramid structured wavelet transform*. Each time the low frequency band is split, the other bands are not touched. This is suitable for signals with most of their energy concentrated in the low frequency regions. However, for some signals, energy is concentrated at the middle frequencies. In this case, we have to split all the bands. This is called *wavelet packet decomposition*. The two-dimensional wavelet packet tree decomposition and the terminology we used are shown (Fig. 2). Letter A represents *approximation*; letters *H*, *V*, and *D* represent *horizontal*, *vertical*, and *diagonal* details, respectively. The left letter is the first, and the right letter is the second decomposition.

4. METHODOLOGY

We can summarize as follows a method that depends on the idea that the performance will increase by decomposing the textile fabric images into their subbands by wavelet transforms as a preprocessing step and applying the three subspace analysis tools, ICA, TICA, and ISA, on these subbands.

The mean of every image is subtracted from itself, and then every image is divided by its variance in order to better condition the ICA (or TICA, or ISA) estimation [12, 13].

A block scheme of the proposed method is given in Fig. 3.

In the off-line block or the learning phase, the independent components for a set of texture images are extracted to be used as the basis vectors in the online block. Once the ICA (or TICA or ISA) basis vectors are calculated, they are used to construct the columns of matrix **A** in the ICA (or TICA or ISA) model. Hence, the columns of **A** represent the ICA (or TICA or ISA) basis vectors. A fix-point algorithm with *tanh* nonlinearity is used to extract the independent components. The number of iterations is taken as 2000 in order to guarantee convergence [14].

The feature vector (which will also be referred to as the coefficient vector) is a vector whose elements are the coefficients of the corresponding independent components. It is calculated for a defect-free image in the off-line part using Eq. (2.3) and is stored as the reference feature vector, $\mathbf{s}_{k,true}$, to be used in the on-line detection part. The subscript k here denotes the corresponding subband. The calculation of the true feature vector, $\mathbf{s}_{k,true}$, can be summarized as follows: After the subwindows of the defect-free image(s) are extracted, the subbands of these image subwindows are decomposed before constructing the data matrix **X**. These subbands are extracted by two-level wavelet transformation. According to the application, one or more subbands can be taken from the possible 16 subbands of the two-level wavelet packet tree scheme. Let K represent the number of subbands taken during the algorithm.

Since two-level wavelet transformation is used, the resulting size of the subband will be $(N/4)$Ç$(N/4)$, where N is the size of the subwindows if no subband analysis is done. This makes the size of each **X** matrix $(N^2/16)$Ç10000. The ith column of the **X** matrix corresponds to the ith subwindow of the corresponding subband. The number of **X** matrices generated depends on the number of subbands used in the analysis. There will be K **X** matrices each corresponding to a different subband of the image subwindows. If only the **AA** subband is used, the ith column of the **X** will be the AA subband of the ith subwindow. Accordingly, other **X** matrices will be constructed for other subbands.

After the data acquisition part, the dimension of the data is reduced to a number that is equal to the number

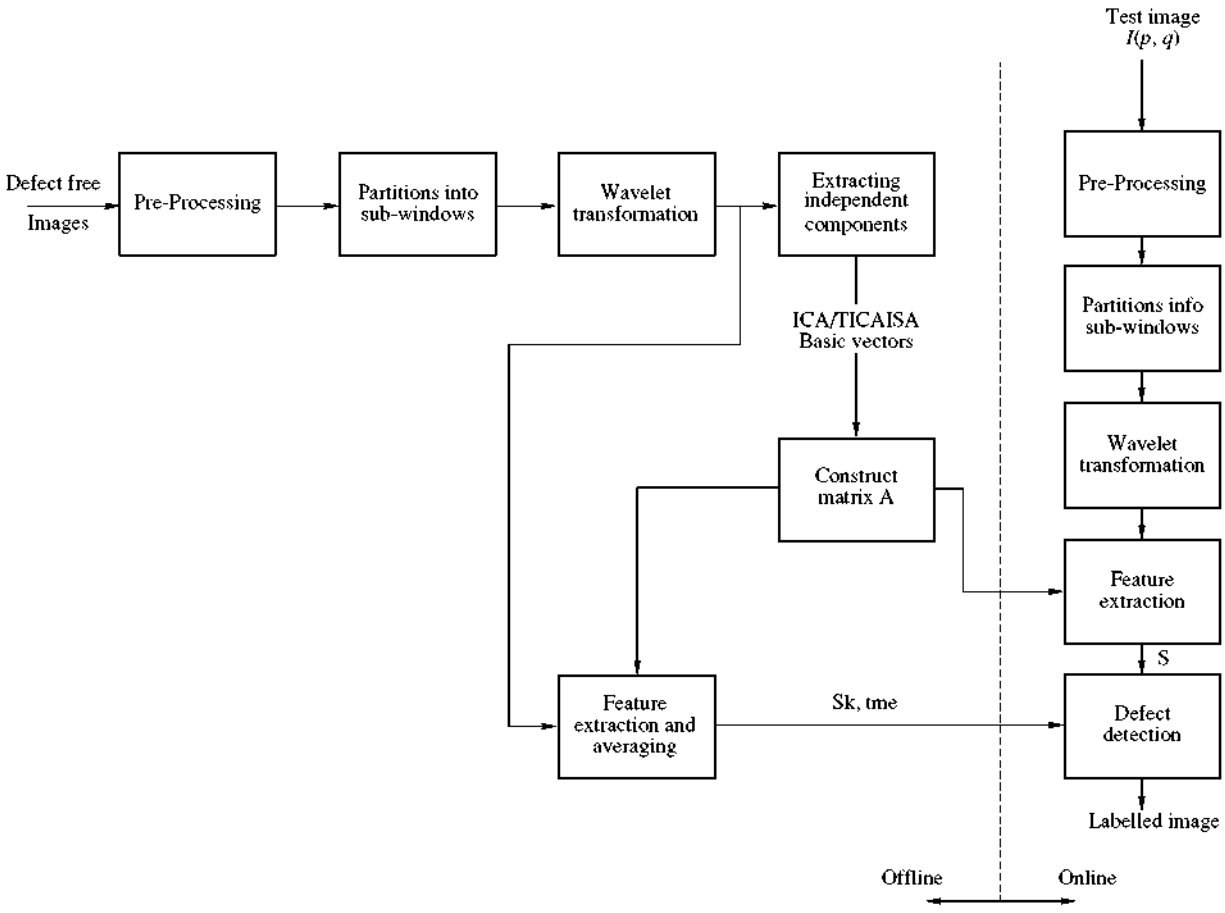

Fig. 3. Proposed defect detection system.

of desired independent components. However, note that, if the dimension has already been reduced to the number of desired independent components by wavelet transform, this step can be skipped without loss of generality. Dimension reduction is performed by PCA to reduce the computation time. If m represents the number of desired independent components, m eigenvectors with the m highest eigenvalues of the covariance matrix of **X** are chosen in PCA.

As mentioned previously, the feature vectors used are the coefficients of the independent components, namely, the s_i's constitute the feature vectors. Feature vectors $\mathbf{s}_{k,i}$ are extracted for the kth subband of the ith subwindow by multiplying the pixel values of the subwindow by the corresponding demixing matrices which are found by the ICA (or TICA, or ISA) algorithm. The demixing matrix is the (pseudo) inverse of the **A** matrix that is constructed in terms of the ICA (or TICA, or ISA) basis vectors in the off-line part. This makes a total of K feature vectors of size m for each subwindow. In order to find the $\mathbf{s}_{k,true}$ vector, which is the true feature vector representing the nondefective regions, the mean of those 10000 feature vectors (coefficients of the independent components) are taken for each subband. This makes a total of K $\mathbf{s}_{true}$ vectors ($\mathbf{s}_{k,true}$), where each true vector corresponds to the appropriate subband used.

In the on-line detection part, the demixing matrix found in the off-line part is used. The image to be tested is divided into NÇN nonoverlapping subwindows making a total of $256^2/N^2$ subwindows, since the size of each fabric image is 256Ç256. Each subband of each subwindow is multiplied by the corresponding demixing matrices, and the related **s** vectors (feature vectors) are obtained. The Euclidian distances between these vectors and the K true feature vectors are computed. If the mean of these K distances is above the threshold value, α, determined using Eq. (4.1), the corresponding subwindow is said to be defective, otherwise it is said to be nondefective. This procedure is done for all the test windows:

$$\alpha = D_m + \eta(D_u - D_l), \tag{4.1}$$

where D_m is the median value of the feature vector of a subwindow, $D_u - D_l = IQR$ (*IQR* is the *inter quartile range*) and η is a constant determined experimentally. η can be found by trial and error or automatically by methods like cross-validation. In the simulations, the

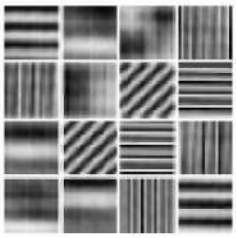

Fig. 4. Independent components of defect free textile fabric images.

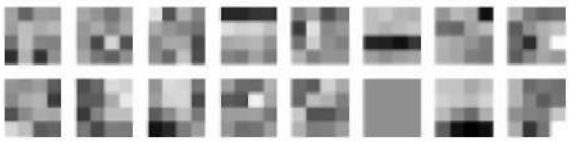

Fig. 5. Sixteen independent components of the (a) AA subband images.

choice of the η value is a compromise to reduce the false alarm rate in defect-free images and to increase the detection rate in defective images.

If wavelet analysis is not used, the formation of the **X** matrix will be performed using the original pixel values of the subwindows of the texture image and there will be one true feature vector $\mathbf{s}_{k,\,true}$ to be used in the online part for defect detection.

The algorithm we use has two basic parameters to be determined: (i) Defect threshold value, α, for each textile type, and (ii) the size of subwindows. The threshold value for best performance can be determined by trial and error for each type of textile separately. It is also important to decide on the appropriate subwindow size for better defect detection performance. The choice of subwindow size depends on two factors [7,]: (i) How localized the defects are, (i.e., size of the defects); the size of the subwindow must be small enough to contain almost only the defect in it; and (ii) for a nondefective sample, how representative of the texture the data is in a window of such size. The subwindow must be large enough to represent the textural properties of the images.

The performance rate of defect detection is calculated by the following formula:

$$\text{Detection Rate } (\%) = 100 \times (N_{CC} + N_{DD})/N_{\text{Total}}, \quad (4.2)$$

where N_{CC} is the number of subwindows being correctly classified as nondefective, N_{DD} is the number of subwindows being correctly classified as defective, and N_{Total} is the total number of subwindows being tested.

5. EXPERIMENTS

The method explained in the previous section is used to detect the weaving defects in textile fabric images. For this purpose, real fabric images were obtained in a laboratory environment by using a CCD camera. Our database contains 36 8-bit grayscale images each 256×256 in size. Sixteen of these images are defect-free, and the others are chosen as to represent the several defect types that may be encountered in the textile industry. Several experiments are conducted in order to assess and compare the defect detection performances of our method. Many different scenarios are generated by using various wavelet transformation methods, different subwindow widths, different numbers of independent components, and several subbands.

The first 13 scenarios rely on the intuition obtained from previous works [27] that, combining the concepts of wavelet transformation and ICA, should increase the defect detection performance in textile images as compared to the performances obtained by applying these methods separately on the same images. Further experiments are performed by applying two other subband analysis tools, TICA and ISA, instead of ICA on the subbands. We used the FastICA algorithm [14], which estimates the independent components by maximizing the nongaussianity.

As a first scenario, defects are detected by using only ICA. In this case, the wavelet transformation block is ignored and ICA is applied on the original subwindows rather than on the subbands of them. Sixteen independent components are extracted with a window size of 16×16. The independent components show the textural properties of the defect free images as shown in Fig. 4. Independent components corresponding to high frequency characteristics show directional properties as vertical, horizontal, and diagonal, and those components corresponding to low frequency characteristics, on the other hand, do not show any directional characteristics, or the directional characteristics are weak.

We then applied subband analysis prior to ICA. The data matrix **X** is formed by the AA subbands of the subwindows. The wavelet transformation is performed by 16-tap Daubachies wavelet filters. Battle–Lemarie wavelet filters, symlets, coiflets, Haar, discrete Meyer, and biorthogonal wavelets were also tried. The best performance is provided by 16-tap Daubachies wavelet filters. Sixteen independent components are extracted, and the subwindow size is taken as 16×16. The performance rate increases by applying subband analysis prior to ICA. We also used the other subbands namely, AH, AV, and AD for subband analysis. With 16 independent components, it is observed that most of the components corresponding to the AH, AV, and AD subbands are composed of zeros which indicates overlearning. Thus, only the independent components corresponding to the AA subband are shown Fig. 5. Since most of the energy is concentrated in the AA band and the energy in the other bands is insignificant, which is also consistent with the findings of Amet et al. [1], the

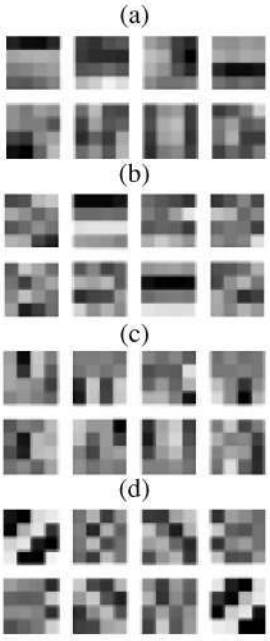

Fig. 6. Eight independent components of the (a) AA; (b) AH; (c) AV; (d)AD subband images.

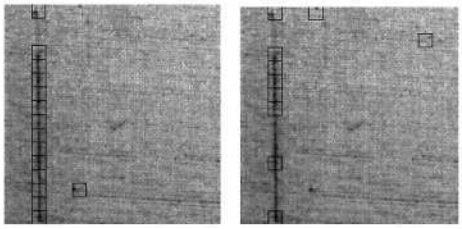

Fig. 8. Intensity defects obtained with 16 independent components by using (a) 1 subband—AA subband, and (b) 4 subbands—AA, AV, AH and AD subbands.

number of significant components corresponding to these bands will be less. A lesser number of components will be sufficient to represent the AH, AV and AD bands; this representation will prevent overlearning. Further dimension reduction by PCA solves this problem as shown in Figs. 6 and 7.

Many reasonable combinations of subbands from the two-level wavelet packet tree scheme have been tried, and the best results are obtained by taking the AA subband since most of the energy is concentrated in this band. This conclusion is consistent with the fact that textile images have low-pass characteristics [1].

It is observed that when only the AA subband is used, better detection rates are attained for intensity defects where the grayscale values of the defective parts are different from those of the overall image. On the other hand, satisfactory defect detection rates for geometrical defects where the textural characteristics are different than those of the general fabric image are obtained when the four subbands, namely, AA, AH, AV

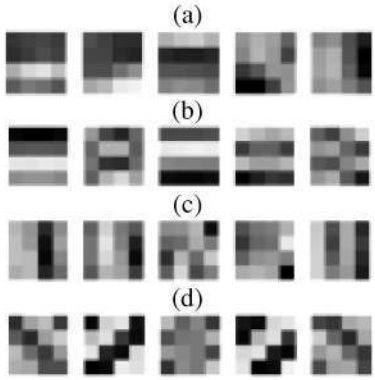

Fig. 7. Five independent components of the (a) AA; (b) AH; (c) AV; (d) AD subband images.

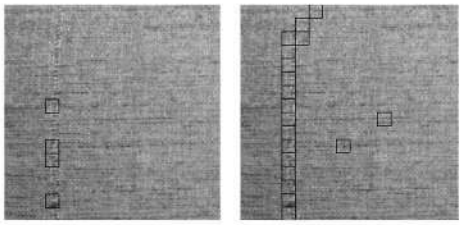

Fig. 9. Geometrical defects obtained with 16 independent components by using (a) 1 subband—AA subband; and (b) 4 subbands—AA, AV, AH and AD subbands.

and AD, are used. This phenomenon can be observed in Figs. 8 and 9, where defect detection is performed both for intensity defects and for geometrical defects, respectively. To increase the overall performance of the system, decision fusion (the logical OR operator) of the results of different subbands are used.

Below is a summary of some of the scenarios that give thorough information about what subband analysis adds upon ICA. The following abbreviations are used for the scenarios.

WS: Window Size.

SB: Number of Subbands.

IC: Number of Independent Components.

ICA: Independent Component Analysis.

W: Wavelet Transform.

WICA: Wavelet applied prior to ICA.

DecFus: Decision Fusion of two methods where in one method only the AA subband is used, and in the other method all the AA, AH, AV, and AD subbands are used.

The scenarios are as follows:

Scenario 1: ICA_16IC_WS16

Scenario 2: WICA_1SB_16IC_WS16

Scenario 3: WICA_4SB_16IC_WS16

Scenario 4: W_1SB_WS16

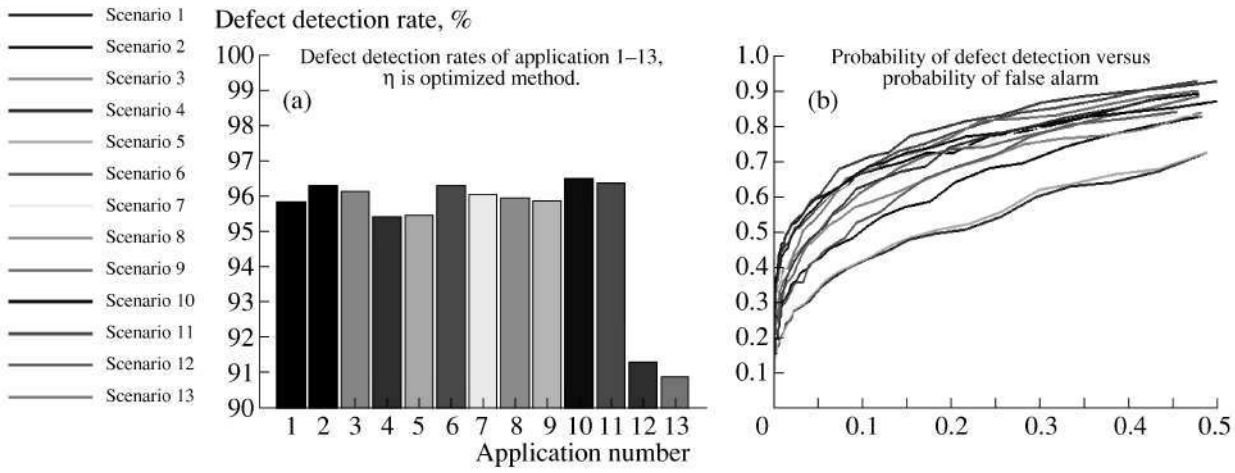

Fig. 10. (a) Defect Detection Rates of Applications; (b) Receiver Operating Curves.

Scenario 5: W_4SB_WS16
Scenario 6: WICA_1SB_8IC_WS16
Scenario 7: WICA_4SB_8IC_WS16
Scenario 8: WICA_1SB_5IC_WS16
Scenario 9: WICA_4SB_5IC_WS16
Scenario 10: DecFus_16IC_WS16
Scenario 11: DecFus_8IC_WS16
Scenario 12: WICA_1SB_8IC_WS32
Scenario 13: WICA_4SB_8IC_WS32

In scenarios 4 and 5, only wavelet transformation (without ICA) is used. In this case, the feature vectors are calculated directly from the energies of the selected subbands. In the last two scenarios, the window size is chosen as 32×32. A comparison of the defect detection rates of all the methods is shown in Fig. 10a. For practical purposes, the η value used in determining the decision threshold given by Eq. (4.1) is optimized for each method. The receiver operating curves (ROCs) are plotted in Fig. 10b for the sake of comparison.

As seen from these experiments, when ICA is applied on the subband images extracted by wavelet transformation tools, the defect detection performance is increased. When the subwindow size is chosen as 16 $\times$ 16 and the number of independent components is chosen as 8, a better performance is obtained compared to the other choices. The best performances are obtained when decision fusion is applied as in scenarios 10 and 11.

Another subspace analysis technique for feature extraction was the use of TICA and ISA. It is observed that these two methods, obtained by relaxing the independence assumption in ICA, lead exactly the same detection rates as ICA. However, it has been observed that they emphasize the directional characteristics of the textures better than ICA does. So, after detecting the defects by ICA, TICA or ISA can be used to classify the defects according to their orientations. For this purpose ISA is found to be a better tool when compared to TICA. The different experiments carried out are detailed below.

The first experiment was to extract 16 independent components to 16 clean images by applying TICA with the standard neighborhood scheme given in Eq. 2.6. The defect detection system described in Fig. 3 is used, where the basis vectors are extracted using TICA. The independent components are shown in Fig. 11.

When we compare the results with those in Fig. 4, we notice that independent components obtained with ICA have some directional behavior. However, this is not the case for components obtained using TICA (see Fig. 11). For example, there are no independent components with diagonal textures in Fig. 11, whereas the orientations of independent components were very obvious in Fig. 4. As mentioned before, the detection rate was the same as ICA. Other topographies have also been tried, but it has been observed that TICA does not add anything on top of ICA in terms of defect detection rate.

ISA has also been tried for feature extraction; however, the same observations were valid; i.e., ISA does not add anything on top of ICA. However, ISA can be used to cluster defect orientations into groups, such as horizontal and vertical. We were inspired by the idea in Li, Lv, and Zhang [21] where they clustered face orien-

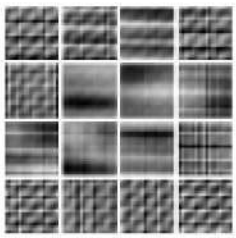

Fig. 11. Sixteen independent components of defect free textile fabric images extracted by TICA, with standard neighborhood scheme.

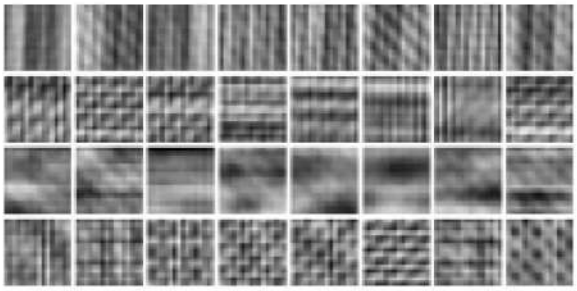

Fig. 12. Four subspace groups, with eight independent components in each, extracted by ISA from defective images.

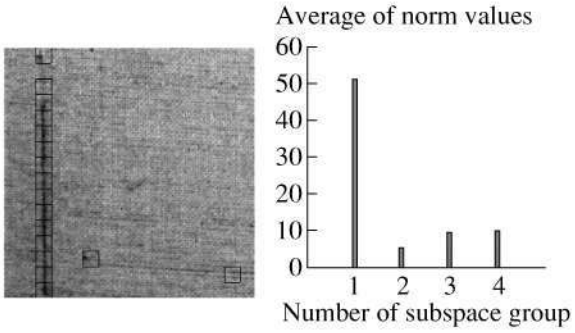

Fig. 13. (a) Defective textile fabric image; (b) Average norms of the four subspace feature vectors extracted from the defective subwindows of the textile image.

tations by using ISA. For the purpose of orientation detection of defects, in the training set, both defective and nondefective samples must be included in order for the system to learn the directions of defects. Many experiments with different numbers of groupings and different numbers of independent components were carried out. Figure 12 shows the four groups and eight independent components in each group.

Once the feature vector **s** is obtained, it is partitioned into four vectors eight in size. Each of the resulting four feature vectors contains the coefficients of the independent components of the corresponding subspace group. The norms of these four feature vectors are compared while deciding on the direction of that subwindow which has been labeled as defective by one of the defect detection algorithms given above.

The four mean values of the norms of the subspaces are plotted next to that figure for all the defective subwindows of the textile fabric image shown in Fig. 13.

As seen in Fig. 13, the average norm corresponding to the first subspace group is much larger than those of the other groups. If we look at Fig. 12, it can be seen that the first group indeed has vertical characteristics. From experiments performed on different images with different defect orientations, it is observed that the subspace group representing the directional characteristics of the defects in a textile fabric image always has the highest energy among other subspace groups.

6. CONCLUSIONS

In this work, a new and efficient defect detection algorithm is developed that combines the concepts of subband domain and subspace analysis methods. This method uses the wavelet transformation as a preprocessing step for the feature extraction problem, which is achieved by subspace analysis tools like ICA, TICA, and ISA. When textures with frequency content mostly concentrated on a single band are considered, focusing on that particular band and discarding the others improves the detection performance. In general, it can be stated that the method applied to subband images is superior to the same method applied to raw images. Since the textural characteristics of geometrical and intensity defects are different, different subbands lead to different detection rates for those classes of defects; thus, decision fusion of the results of different subbands may be a solution to increase the detection performances.

The performances of TICA and ISA where the independence assumption of the independent components are relaxed were not superior of that of ICA. On the other hand, it is shown that ISA is a powerful tool for characterizing the orientations of the defects after they are detected by a certain powerful defect detection algorithm. This is a further step to defect detection, because not only the defects but their orientations can also be detected. It can be said that ISA is a method to classify the defects according to their directionalities.

Considering the results obtained, the new approach seems to be a feasible method for real-time factory implementations.

REFERENCES

1. L. A., Amet, A. Ertuzun, and A. Erçil, "An Efficient Method for Texture Defect Detection: Subband Domain Cooccurrence Matrices," Image and Vision Computing, **18**, 543–553, (2000).
2. A. Atalay, *Automated Defect Inspection of Textile Fabrics Using Machine Vision Techniques,* M.S. Thesis (Bogazici University, Istanbul, Turkey, 1995).
3. A. Bodnarova, M. Bennamoun, and S. J. Latham, "Constrained Minimisation Approach to Optimise Gabor Filters for Detecting Flaws in Woven Textiles," in *Proceedings of the IEEE International Conference on Acoustics, Speech and Signal Processing, ICASSP2000* (Istanbul, Turkey, May 2000), pp. 3606–3609.
4. J. F. Cardoso, "Multidimensional Independent Component Analysis," in *Proceedings of the IEEE,* (1998), no. 10, pp. 2009–2025.
5. C.–H. Chan and K. H. Pang, "Fabric Defect Detection by Fourier Analysis," IEEE Trans. Industry Applications, **36**, 1267–1276 (2000).

6. J. Chen and A.K. Jain, "A Structural Approach to Identify Defects in Textural Images," in *Proceedings IEEE International Conf. Systems, Man and Cybernetics* (Beijing, 1988), pp. 29–32.
7. F. S. Cohen, Z. Fan, and S. Attali, "Automated Inspection of Textile Fabrics Using Textural Models," IEEE Transactions on Pattern Analysis and Machine Intelligence, **13**, no. 8, 803–808, August, (1991).
8. I. Daubechies, "Orthonormal Bases of Compactly Supported Wavelets," Communications on Pure and Applied Mathematics, **41**, 909–996, November, (1988).
9. P. Dewaele, P. Van Gool, and A. Oosterlinchk, "Texture Inspection with Self-Adaptive Convolution Filters," in *Proceedings 9th ICPR* (Rome, Italy, 1988, November 14–17), pp. 56–60.
10. A. Ercil and B. Ozuyılmaz, "Automated Visual Inspection of Metallic Surfaces," in *Proceedings the Third International Conference on Automation, Robotics and Computer Vision, (ICARCV'94)*, (Singapore, November 1994), pp. 1950–1954.
11. J. Hurri, *Independent Component Analysis of Image Data*, MS Thesis, (Helsinki University of Technology, Espoo, Finland, 1997).
12. A. Hyvarinen, "Survey on Independent Component Analysis," Neural Computing Surveys, no. 2, 94–128 (1999).
13. A. Hyvarinen,and E. Oja, "Independent Component Analysis: Algorithms and Applications," Neural Networks, **13**, no. 4–5, 11–430 (2000).
14. A. Hyvarinen and E. Oja, "A Fast Fixed-Point Algorithm for Independent Component Analysis," Neural Computation, **9**, no. 7, 1483–1492, (1997).
15. A. Hyvarinen, and P. O. Hoyer, "Emergence of Phase and Shift Invariant Features by Decomposition of Natural Images into Independent Feature Subspaces," Neural Computation, **12**, no. 7, 1705–1720 (2000).
16. A. Hyvarinen, P. O. Hoyer, and M. Inki, "Topographic Independent Component Analysis," Neural Computation, **13**, 1527—1558 (2001).
17. J. Iivarinen, "Surface Defect Detection with Histogram-Based Texture Features," in *Proceedings SPIE 4197* (2000), pp. 140–145.
18. D. A. Karras, S. A. Karkanis, D. K. Iakovidis, D. E. Maroulis, and B. G. Mertzios, "Improved Defect Detection in Manufacturing Using Novel Multidimensional Wavelet Feature Extraction Involving Vector Quantization and PCA Techniques," in *Proceedings 8th Panhellenic Conference on Informatics* (Nicosia, Cyprus, 2001, Nov. 7–10).
19. T. Kohonen, "Emergence of Invariant-Feature Detectors in Adaptive-Subspace Self-Organizing Map," Biological Cybernetics, **75**, 281–291 (1996).
20. G. Lambert and F. Bock, "Wavelet Methods for Texture Defect Detection," in *Proceedings of the IEEE International Conference on Image Processing* (1997), vol. 3, pp. 201–204.
21. S. Z. Li, X. Lv, and H. Zhang, "View Based Clustering of Object Appearances Based on Independent Subspace Analysis," in *Proceedings Eighth IEEE International Conference on Computer Vision (ICCV 2001)* (Vancouver, BC, Canada, 7–14 July 2001), pp. 295–300.
22. S. G. Mallat, "A Theory for Multiresolution Signal Decomposition: The Wavelet Representation," IEEE Transactions on Pattern Analysis and Machine Intelligence, **11**, no. 7, 674–693, July (1989).
23. R. Meylani, *Texture Analysis Using Adaptive Two-Dimensional Lattice Filters*, MS Thesis (Bogazici University, Istanbul, Turkey, 1997).
24. R. Meylani, A. Ertuzun, and A. Ercil, "A Comparative Study on the Adaptive Lattice Structures in the Context of Texture Defect Detection," in *Proceedings ICECS 96* (Rhodes, Greece, 1996, October 13–16), vol. 2, pp. 976–979.
25. A. R. Rao, *A Taxonomy for Texture Description and Identification*, Springer-Verlag, New York, 1990).
26. T. R. Reed, and J. M. Hans Du Buf, "A Review of Recent Texture Segmentation and Feature Extraction Techniques," CVGIP: Image Understanding, **57**, 359–372 (1993).
27. A. Serdaroglu, A. Ertuzun, and A. Ercil, "Defect Detection in Textile Fabric Images Using Wavelet Transforms and Independent Component Analysis," *Pattern Recognition and Image Understanding: New Technologies, PRIA–7–2004* (St. Petersburg, Russian Federation, 2004, Oct. 18–23).
28. O. G. Sezer, A. Ertuzun and A. Ercil, "Independent Component Analysis for Texture Defect Detection," Pattern Recognition and Image Analysis, **14**, no. 2, 303–307 (2004).
29. O. G. Sezer, A. Ertuzun, and A. Ercil, "Using Perceptual Relation of Regularity And Anisotropy in the Texture with Independent Component Model for Defect Detection," Submitted to Pattern Recognition.
30. M. Tuceryan and A. Jain, "Texture Analysis," in *The Handbook of Pattern Recognition and Computer Vision*, Eds. by C. H. Chen, L. F. Pau, and P. S. P. Wang, (World Scientific Publishing Co., 1993).
31. L. Van Gool, P. Dewaele, and A. Oosterlinck, "Survey-Texture Analysis Anno 1983," Computer Vision, Graphics and Image Processing, **29**, 336–357 (1985).
32. L. Xu, "Least Mean Square Error Reconstruction Principle for Self-Organizing Neural Nets," Neural Networks, no. 6, 627–648 (1993).

Ayşin Ertuzun. Born 1959 in Salihli, Turkey. Received the BS degree (with honors) from Boğaziçi University, Istanbul, Turkey, MA (Eng.) degree from McMaster University, Hamilton, Ontario, Canada, and the PhD from Boğaziçi University, Istanbul, Turkey, all in electrical engineering, in 1981, 1984 and 1989, respectively. Since 1988, she is with the Department of Electrical and Electronic Engineering at Boğaziçi University, where she is currently an associate professor.

Her current research interests are in the areas of bling signal processing, Bayesian methods, adaptive systems and filtering with applications to communication systems, image processing, independent component analysis and its applications and pattern recognition.

She has authored and coauthored nearly 50 scientific papers in journals and conference proceedings.

She is a member of IEEE and IAPR.

Ahmed Serdaroglu. Born in 1981 in Lingen, Germany. Received BS degree (with high honors) from Boğaziçi University, Istanbul, Turkey, in July 2004. Since September 2004, he is with the Department of Electrical, Computer, and Systems Engineering at Rensselaer Polytechnic Institute (RPI), Troy, New York. Currently, he is a graduate research assistant at RPI

His current research interests are Fluorescence Diffuse Optical Tomography, Bayesian estimation, mathematical inverse problems encountered especially in biomedical engineering aplications, and pattern recognition.

Aytül Ercil. Born December 14, 1958. Received her BS degrees in electrical engineering and mathematics from Boğaziçi University, Istanbul, Turkey in 1979; MS and PhD degrees in applied mathematics from Brown University, United States, in 1980 and 1983, respectively. She worked at GM Research Laboratories, Michigan, United States, as a senior research scientist and staff research scientist until 1988. She has tought at Boğaziçi University, Turkey, and has been a technical consultant to various organizations. She is currently a professor at the Faculty of Engineering at Sabancı University, Istanbul, Turkey, and the director of VPA-LAB—Computer Vision and Pattern Recognition Lab at the same university.

She has directed many national and international research projects and has over 100 publications.

Her research topics include invariant objects recognition, shape modeling, texture analysis, pattern recognition, and biometrics.

President of TÖTİAD—Turkish Pattern Recognition and Image Processing.

SPELL: 1. cooccurrence, 2. Iivarinen, 3. cooccurence, 4. denoising, 5. invariances, 6. prewhitening, 7. upsampled, 8. online, 9. tme, 10. Offline